Akaike Causality in State Space
Part I - Instantaneous Causality Between Visual Cortex in fMRI Time Series

K.F. Kevin Wong, Tohru Ozaki

December 21, 2006

Abstract

We present a new approach of explaining partial causality in multivariate fMRI time series by a state space model. A given single time series can be divided into two noise-driven processes, which comprising a homogeneous process shared among multivariate time series and a particular process refining the homogeneous process. Causality map is drawn using Akaike noise contribution ratio theory, by assuming that noises are independent. The method is illustrated by an application to fMRI data recorded under visual stimulus.

Keywords: Akaike causality, noise contribution ratio, state space model, common source, partial causality, functional MRI, primary visual cortex, middle temporal cortex, posterior parietal cortex.

1 Introduction

For the purpose of causality analysis in multivariate time series data Akaike (1968) decomposes power spectral density into components, each coming from an independent noise of multivariate autoregressive model (VAR). Controversy on Akaike noise contribution ratio (NCR) causality mainly focuses on the validity of causality when residuals are spatially highly correlated, that phenomenon can be reflected from large covariance entry in noise covariance matrix. When driving noises have a high correlation instantaneously, independence assumption of noise is not adequate, a non-zero noise covariance is essential to improve the time series model. This indispensable covariance suggests that two corresponding time series are driven by similar noises, which apparently showing causal relationship instantaneously from one to the other, without a clue who is causing whom.

The causality being discussed is known to be *instantaneous causality.* Geweke (1982) tested the likelihood ratio in order to decide the significance of instantaneous causality. One deficiency is an unclear cut of causality when the model order is getting high, so that feedback of instantaneous causality through autoregressive process occurs and instantaneous causality plays a role more than just instantaneously.

We propose an alternative way to look at the instantaneous causality by state space model (Wong, 2005). In particular, we assume, instead of in-directed causality between two variables, a directed causality from a latent variable to the two variables. We will model the fMRI by a linear autoregressive model plus a homogeneous variable in a state space framework.

2 fMRI data under visual stimulus

The data selected as an example to illustrate our new method is obtained from a recent research of Yamashita et al. (2005). The time series of BOLD signal of a healthy subject under a visual stimulation was obtained in an fMRI scanning machine. A black screen is presented to the subject for 30 seconds, then white dots appeared on the black screen and flew outwards from center of the screen for 30 seconds. The two screens switched in every 30 seconds. A detailed experimental procedure and pre-processing procedure can be found in Yamashita et al. (2005).

Yamashita et al. (2005) selected three regions of interest, primary visual cortex (V1), visual cortex area 5 (V5) and posterior parietal cortex (PP). They are reported to respond to human attention to visual motion. (Büchel & Friston, 1997) The primary visual cortex (V1) is an entrance of visual stimuli. Through V1 information is further transmitted to other visual areas, such as visual areas V2, V3, V4 and V5. The visual area V5, also known as visual area MT (middle temporal), is a region of extrastriate visual cortex that is thought to play a major role in the perception of motion. Posterior parietal cortex (PP) is another distinctive cortical area appearing to be important for spatial processing and the control of eye movements, may also have a central role in visual attention. We are interested in how is connectivity among these areas in responding to visual stimulus.

In figure 1 we show the time series data on a time axis in second. The data set contains four discontinuous segments. Each segment has 270 time points covering 270 seconds. Yamashita et al. (2005) analyzed the time series by VAR and adding the information of onset of stimulus as an exogenous variable to the model. They reported that strong connectivity exists from V1 to V5 and from V5 to PP at a period of 60 seconds, which is the time between starting time of two consecutive stimuli.

3 Method and Result

We intend to fit the time series to a state space model and plot a causality map based on the model. A latent variable is included in state vector in

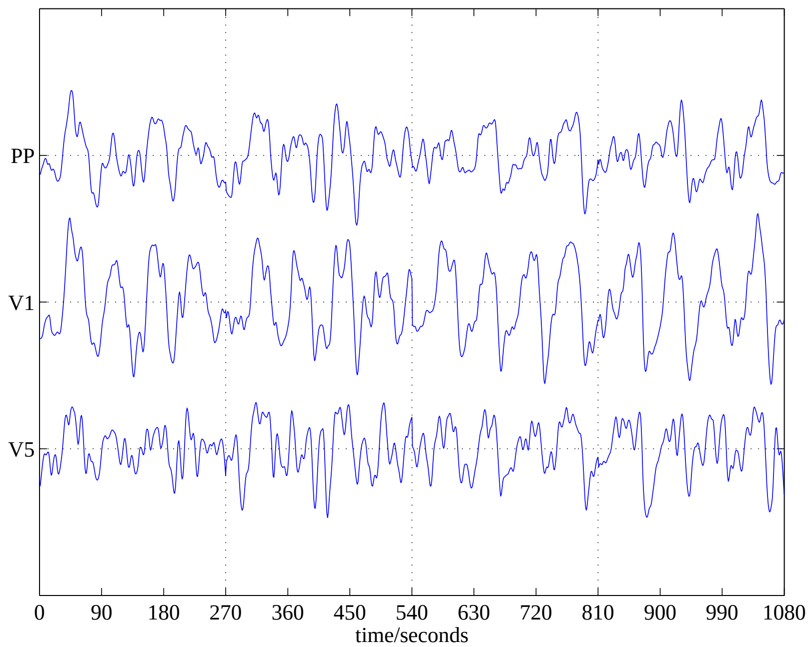

Figure 1: fMRI BOLD signals under visual stimuli

order to get rid of a common dynamic which is driving the three cortex areas simultaneously. Nevertheless, three individual driving noises representing corresponding cortex areas pertain mutual causality, through a feedback system provided by a transition matrix.

Let y_t denote the observed data and x_t the unobserved state. We assume that x_t depends on its past values through a linear stochastic model, containing a dynamical noise term, and that y_t follows from x_t through a linear observation model, containing an observation noise term; then the following state space model applies:

$$\boldsymbol{x}_t = F\boldsymbol{x}_{t-1} + G\boldsymbol{w}_t \quad (1)$$

$$\boldsymbol{y}_t = H\boldsymbol{x}_t + \epsilon_t \quad (2)$$

Equations (1) and (2) are commonly known as system equation and observation equation, respectively. w_t denotes the dynamical noise term of the system equation, assumed to follow a multivariate Gaussian distribution $w_t \sim N(0, Q_t)$, while ϵ_t denotes the observation noise term of the observation equation, assumed to follow a univariate Gaussian distribution $\epsilon_t \sim N(0, R)$.

Kalman (1960) introduced a filtering technique for state space models which can efficiently calculate the conditional prediction and conditional filtered estimation of unobserved states. A comprehensive introduction to state space models and Kalman filtering has been provided by Kalman (1960), Harrison & Stevens (1976), Harvey (1989), Grewal & Andrews (2001).

Since we aim at decomposing the time series into a common source component and a particular source component, we choose a special structure for the state space model, such that the last element of the state vector x_t represents the common source component, and the former elements of the vector form a 3-variate AR model. By this we should have a canonical form (Aoki, 1990) for the 3-variate AR and a coefficient for the common source along the diagonal of F. The 3-variate AR should capture main characteristics of the time series but the common source should only capture instantaneous and simultaneous dynamic, therefore the coefficient for the common source should be small, for instance 0.05.

The model parameters in Equations (1) and (2) are estimated from given data by the maximum-likelihood method. Given a set of parameters, computation of the likelihood from the errors of the data prediction through application of the Kalman filter is straightforward; see Mehra (1971), Åström & Kallstrom (1973), Sorenson (1985) and Valdés-Sosa et al. (1999) for a detailed treatment. A maximum likelihood estimate for the state space model is as follows.

$$F = \begin{bmatrix} 3.0165 & 0.1486 & -0.0516 & 1 & 0 & 0 & 0 & 0 & 0 & 0 & 0 & 0 & 1 \\ 0.0414 & 3.1754 & 0.0023 & 0 & 1 & 0 & 0 & 0 & 0 & 0 & 0 & 0 & 1.1335 \\ 0.0246 & 0.0690 & 3.1140 & 0 & 0 & 1 & 0 & 0 & 0 & 0 & 0 & 0 & 0.9725 \\ -3.6868 & -0.3493 & 0.0693 & 0 & 0 & 0 & 1 & 0 & 0 & 0 & 0 & 0 & 0 \\ -0.0307 & -4.0918 & 0.0083 & 0 & 0 & 0 & 0 & 1 & 0 & 0 & 0 & 0 & 0 \\ 0.0236 & -0.1487 & -4.0049 & 0 & 0 & 0 & 0 & 0 & 1 & 0 & 0 & 0 & 0 \\ 2.2126 & 0.2975 & -0.0214 & 0 & 0 & 0 & 0 & 0 & 0 & 1 & 0 & 0 & 0 \\ -0.0451 & 2.5811 & -0.0089 & 0 & 0 & 0 & 0 & 0 & 0 & 0 & 1 & 0 & 0 \\ -0.0801 & 0.1102 & 2.5351 & 0 & 0 & 0 & 0 & 0 & 0 & 0 & 0 & 1 & 0 \\ -0.5601 & -0.0873 & -0.0069 & 0 & 0 & 0 & 0 & 0 & 0 & 0 & 0 & 0 & 0 \\ 0.0348 & -0.6735 & -0.0007 & 0 & 0 & 0 & 0 & 0 & 0 & 0 & 0 & 0 & 0 \\ 0.0348 & -0.0219 & -0.6720 & 0 & 0 & 0 & 0 & 0 & 0 & 0 & 0 & 0 & 0 \\ 0 & 0 & 0 & 0 & 0 & 0 & 0 & 0 & 0 & 0 & 0 & 0 & 0.0500 \end{bmatrix},$$

$$G = \begin{bmatrix} 1 & 0 & 0 & 0 \\ 0 & 1 & 0 & 0 \\ 0 & 0 & 1 & 0 \\ 0 & 0 & 0 & 0 \\ \vdots & \vdots & \vdots & \vdots \\ 0 & 0 & 0 & 0 \\ 0 & 0 & 0 & 1 \end{bmatrix}, \quad H = \begin{bmatrix} 1 & 0 & 0 & 0 & \dots & 0 \\ 0 & 1 & 0 & 0 & \dots & 0 \\ 0 & 0 & 1 & 0 & \dots & 0 \end{bmatrix},$$

$$Q = \begin{bmatrix} 0.0460 & 0 & 0 & 0 \\ 0 & 0.0515 & 0 & 0 \\ 0 & 0 & 0.0631 & 0 \\ 0 & 0 & 0 & 0.0335 \end{bmatrix},$$

$$R = \begin{bmatrix} 0 & 0 & 0 \\ 0 & 0 & 0 \\ 0 & 0 & 0 \end{bmatrix}.$$

Akaike information criterion(AIC), a value for comparing statistical models by weighing likelihood function and number of model parameters, is 965.3 (= 879.3 + 2 × 43) for the state space model, comparing to 984.4 (= 900.4 + 2 × 42) for a VAR(4) with full matrix of noise variance. It suggests that the state space model should be a more suitable model to the time series.

In figure 2(a) we show the spectra of fMRI of, from left to right, PP, V1 and V5, based on the estimated state space model. Each spectrum is constituted of 4 colors, which corresponding to 4 system noises of the state space model. By the state space structure we have already assume green, red, yellow and black are respectively PP, V1, V5 and common source. Through F, G and H, the 4 noises contribute to the time series distinctively, showed by the model spectra. Among the 3 spectra, the one of V1 has the

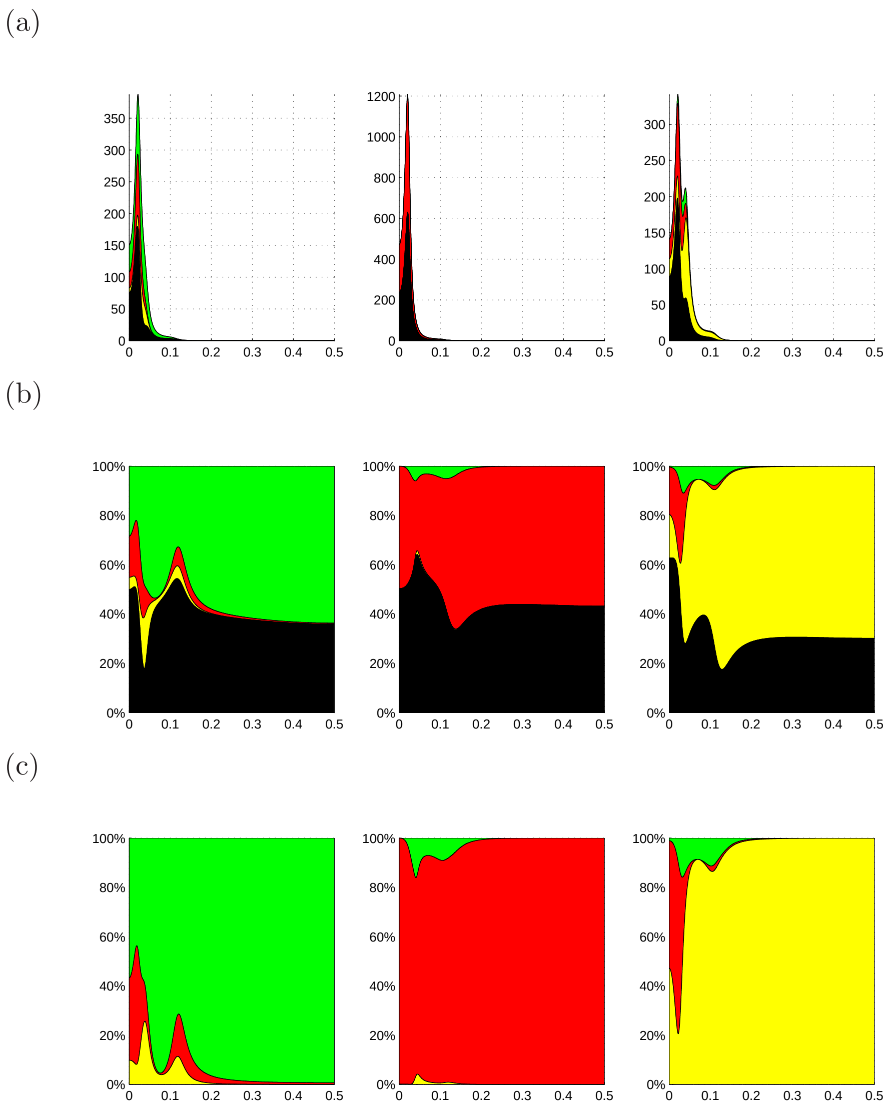

Figure 2: Model spectra, NCR causality map and partial NCR causality map of state space

highest power intensity at around 0.02, about 50-second period oscillation, which can also be seen clearly from the data.

In figure 2(b) we show the NCR causality map, which obtained by normalizing the spectra in (a). At each frequency the spectral power intensity is squeezed into 0% to 100%, so that the ratio of contribution from each noise variance can be seen clearly at each frequency. Since most power intensity is dense between 0 to 0.06 interval, we shall explain causality based on this interval. The black color is the noise in driving the time series simultaneously by assumption. We can see this common source explains over 50% of power intensity at 0Hz in all the spectra. Also, it has shared over 50% of power intensity of the lower frequency region of V1. Note that this common source has been introduced to the state space model through an AR process of coefficient 0.05, which meaning this noise is not providing an additional degree of characteristic root to the transition matrix, but sparing more room for the correlated residuals from AR.

In figure 2(c) we show the partial NCR causality map, when the contribution of common source, ie black, is eliminated. These remaining colors can tell the causality from these independent noises to the time series. V1 is showing up around low frequency range, saying that causality from V1 to PP and V5 is significant. PP is causing V1 and V5 a little, mostly at the neighborhood of 0.5 (20-25s period oscillation), and at the same time, V5 is causing PP a little and V1 negligibly nothing.

We compare the above result to the causality result from AR, of which noise variance matrix is diagonal, estimated by least square method. AIC of an AR(4) with diagonal noise variance is 1452.7 (= 1374.7 + 2 × 39), a value much greater than the AIC of state space model, meaning this AR(4) is less suitable to the time series.

$$
\begin{aligned}
\begin{pmatrix} y_t^{(1)} \\ y_t^{(2)} \end{pmatrix} &= \begin{pmatrix} 3.0183 & 0.1499 & -0.0504 \\ 0.0433 & 3.1768 & 0.0036 \\ 0.0262 & 0.0701 & 3.1151 \end{pmatrix} \begin{pmatrix} y_{t-1}^{(1)} \\ y_{t-1}^{(2)} \\ y_{t-1}^{(3)} \end{pmatrix} \\
&+ \begin{pmatrix} -3.6896 & -0.3517 & 0.0674 \\ -0.0337 & -4.0944 & 0.0063 \\ 0.0212 & -0.1507 & -4.0064 \end{pmatrix} \begin{pmatrix} y_{t-2}^{(1)} \\ y_{t-2}^{(2)} \\ y_{t-2}^{(3)} \end{pmatrix} \\
&+ \begin{pmatrix} 2.2126 & 0.2985 & -0.0205 \\ -0.0453 & 2.5821 & -0.0080 \\ -0.0805 & 0.1108 & 2.5357 \end{pmatrix} \begin{pmatrix} y_{t-3}^{(1)} \\ y_{t-3}^{(2)} \\ y_{t-3}^{(3)} \end{pmatrix} \\
&+ \begin{pmatrix} -0.5589 & -0.0873 & -0.0070 \\ 0.0362 & -0.6734 & -0.0008 \\ 0.0360 & -0.0217 & -0.6720 \end{pmatrix} \begin{pmatrix} y_{t-4}^{(1)} \\ y_{t-4}^{(2)} \\ y_{t-4}^{(3)} \end{pmatrix} + \begin{pmatrix} \eta_t^{(1)} \\ \eta_t^{(2)} \\ \eta_t^{(3)} \end{pmatrix}
\end{aligned}
$$

$$\begin{pmatrix} \eta_t^{(1)} \\ \eta_t^{(2)} \\ \eta_t^{(3)} \end{pmatrix} \sim \mathrm{N}\left(\begin{pmatrix} 0 \\ 0 \\ 0 \end{pmatrix}, \begin{pmatrix} 0.0797 & 0 & 0 \\ 0 & 0.0948 & 0 \\ 0 & 0 & 0.0949 \end{pmatrix} \right)$$

By this AR(4) we plot model spectra in figure 3(a) and NCR causality map in figure 3(b). To our surprise this NCR causality map is so similar to that in Figure 2(b). On one hand it has proven that the common source component was added to lessen the squares of residual but not to take away any model characteristics by our assumption, and on the other hand we can assure our result in state space is consistent.

(a)

(b)

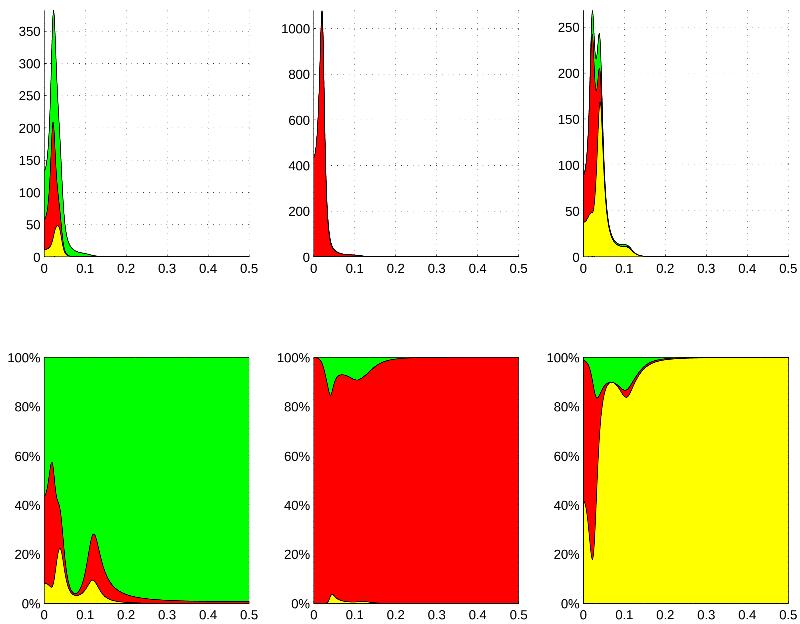

Figure 3: Model spectra and NCR causality map

4 Discussion

We proposed a new method to apply Akaike causality in state space framework so that the only limitation of Akaike causality is solved when residuals of VAR is highly correlated. Correlation between noises in VAR is sorted out as an additional independent noise homogeneously driving multivariate time series in a state space framework. By comparing the AIC we found that the state space model fits better than the VAR.

The idea in this paper can be further extended. Besides a common source component for all time series, some pairwise or tuple-wise common source components can be added into the model. For instance in this paper, in additional to the common source of black color, we can introduce one more color for a common source of V1 and V5 but not PP, so that the common source with the visual cortex can be further eliminated. More generally we should add also the other two combinations of pairwise common source components.

However, time series in real application often share common characteristics. A common characteristics greatly shared by two time series may also appear in other time series, that it should not be negligibly zero even though its strength is small. Therefore pairwise common variables could be easily absorbed by an overall homogeneous variable. See Tanokura & Kitagawa (2003) for a similar treatment.

Like any other causality theory, Akaike causality has to be based on a model. The goodness of an estimated model affects very much the causality conclusion. Therefore, before drawing any causality conclusion, much effort on finding a suitable model is necessary.

5 Appendix

5.1 State space model and its ARMA representation

Here we will give the ARMA representation of state space model. Referring to Equation (1) and (2), let F, G and H are of size $m \times m$, $m \times k$ and $\ell \times m$ respectively. Then F has m eigenvalues, thus there is a characteristic polynomial of order m, so that we can transform F linearly to zero by Cayley Hamilton Theorem.

$$F^m - \phi_1 F^{m-1} - \phi_2 F^{m-2} - \cdots - \phi_{m-1} F - \phi_m I \quad = \quad 0 \ .$$

By this a linear state space model can be transformed to a VARMA in terms of observed data $\boldsymbol{y}$ and noises η.

$$\begin{aligned} &\boldsymbol{y}_t - \phi_1 \boldsymbol{y}_{t-1} - \phi_2 \boldsymbol{y}_{t-2} - \cdots - \phi_m \boldsymbol{y}_{t-m} \equiv \\ &\qquad \Theta_0 \eta_t + \Theta_1 \eta_{t-1} + \Theta_2 \eta_{t-2} + \cdots + \Theta_{m-1} \eta_{t-m+1} + \Theta_m \eta_{t-m} \end{aligned} \tag{3}$$

Let I be identity matrix.

$$\begin{aligned} \Theta_0 &= \left(\ HG \mid I \ \right) \\ \Theta_1 &= \left(\ H(F - \phi_1 I) G \mid -\phi_1 I \ \right) \\ \Theta_2 &= \left(\ H\left(F^2 - \phi_1 F - \phi_2 I\right) G \mid -\phi_2 I \ \right) \\ &\vdots \\ \Theta_{m-1} &= \left(\ H\left(F^{m-1} - \phi_1 F^{m-2} - \cdots - \phi_{m-2} F - \phi_{m-1} I\right) G \mid -\phi_{m-1} I \ \right) \\ \Theta_m &= \left(\ 0 \mid -\phi_m I \ \right) \\ \eta_{t-j} &= \begin{pmatrix} \boldsymbol{w}_{t-j} \\ \epsilon_{t-j} \end{pmatrix} \sim N(0, \Sigma), \Sigma = \begin{pmatrix} Q & 0 \\ 0 & R \end{pmatrix} \end{aligned}$$

Autoregressive coefficients of the VARMA are scalars which are coefficients of the characteristic equation of F. Moving average coefficients Θ are formed by two block matrices, of sizes $\ell \times k$ and $\ell \times \ell$, which depend on F, G and H only. This noise vector η is stacked by $\boldsymbol{w}_t$ and ϵ_t vertically. Note that the size of η is not necessary as same as that of $\boldsymbol{y}$. Although the autoregressive part is molded identically for all variables in $\boldsymbol{y}$, the moving average part refines each variable uniquely.

5.2 Akaike causality for VARMA and State Space

Here we will give derivation of Akaike causality of VARMA only. Akaike causality for state space is straightforward by combining this result with the formula in the previous subsection.

By Equation 3 we will obtain a power spectral density matrix P_f for a VARMA.

$$\begin{aligned} \mathcal{F}_f(\Phi) &= -I + \sum_{j=1}^{p} \Phi_j e^{-2ji\pi f}, \qquad \mathcal{F}_f(\Theta) = \sum_{j=0}^{q} \Theta_j e^{-2ji\pi f}, \\ P_f &= \mathcal{F}_f(\Phi)^{-1} \mathcal{F}_f(\Theta) \Sigma \mathcal{F}_f(\Theta)^H \left\{ \mathcal{F}_f(\Phi)^{-1} \right\}^H . \end{aligned}$$

At each frequency f, the diagonal elements of P_f are spectral density of time series and the off-diagonal elements are cross spectral density. If Σ is a diagonal matrix, each diagonal elements of P_f is weighted sum of the diagonals of Σ. By this Akaike NCR causality is defined by the proportion of power from one noise variance to the power from all noise variance.

$$\mathrm{NCR}\left(\sigma^2, y_t\right) = \frac{\text{spectral density going to } y_t \text{ from } \sigma^2}{\text{total spectral density going to } y_t \text{ from all variances}}$$

Acknowledgements

The authors would like to thank Dr Okito Yamashita and Prof Norihiro Sadato for providing the fMRI data, and special thanks to Prof Rolando Biscay for his comments and guidance.

This work was supported by the Atsumi International Scholarship Foundation, the Iwatani Naoji Foundation, Research Institute of Science and Technology for Society of the Japan Science and Technology Agency and the Japanese Society for the Promotion of Science through Kiban B *no. 173000922301*.

References

Akaike, H. (1968). On the use of a linear model for the identification of feedback systems. *Annals of the Institute of Statistical Mathematics* 20 425–439.

Aoki, M. (1990). *State Space Modeling of Time Series*. New York: Springer-Verlag.

Åström, K. J. & Kallstrom, C. G. (1973). Application of system identification techniques to the determination of ship dynamics. In P. Eykhoff, ed., *Identification and system parameter estimation*. Amsterdam: North-Holland.

Büchel, C. & Friston, K. J. (1997). Modulation of connectivity in visual pathways by attention: Cortical interactions evaluated with structural equation modelling and fMRI. *Cereb. Cortex* 7 768–778.

Geweke, J. F. (1982). Measurement of linear dependence and feedback between multiple time series. *Journal of the American Statistical Association* 77 304–324.

Grewal, M. S. & Andrews, A. P. (2001). *Kalman filtering: Theory and Practice Using MATLAB 2nd edition*. New York: Wiley.

Harrison, J. & Stevens, C. F. (1976). Bayesian forecasting (with discussion). *Journal of the Royal Statistical Society, Series B* 38 205–247.

Harvey, A. C. (1989). *Forecasting, structural time series models and the Kalman filter*. Cambridge: Cambridge University Press.

Kalman, R. E. (1960). A new approach to linear filtering and prediction problems. *Journal of Basic Engineering* 82 35–45.

Mehra, R. K. (1971). Identification of stochastic linear dynamic systems. *American Institute of Aeronautics and Astronautics Journal* 9 28–31.

Sorenson, H. W. (1985). *Kalman Filtering: Theory and Application*. IEEE Press.

Tanokura, Y. & Kitagawa, G. (2003). Extended power contribution that can be applied without independence assumption. Tech. Rep. 886, The Institute of Statistical Mathematics.

Valdés-Sosa, P., Jimenez, J. C., Riera, J., Biscay, R. & Ozaki, T. (1999). Nonlinear EEG analysis based on a neural mass model. *Biological Cybernetics* 81 348–358.

Wong, K. F. K. (2005). *Multivariate Time Series Analysis of Heteroscedastic Data with Application to Neuroscience*. Ph.D. thesis, Graduate University for Advanced Studies.

Yamashita, O., Sadato, N., Okada, N. & Ozaki, T. (2005). Evaluating frequency-wise directed connectivity of bold signals applying relative power contribution with the linear multivariate time series models. *Neuroimage* 25 478–490.